

A Covariant OBE Model for η Production in NN Collisions

E.Gedalin,^{*} A.Moalem[†] and L.Razdolskaja[‡]

Department of Physics
Ben-Gurion University of the Negev
Beer-Sheva, 84105, Israel

PACS numbers:25.40Ve, 13.75Cs,14.40Aq

Keywords:eta meson production, Coivariant OBE model

^{*}gedal@bgumail.bgu.ac.il

[†]moalem @bgumail.bgu.ac.il

[‡]ljuba@bgumail.bgu.ac.il

Abstract

A relativistic covariant one boson exchange model, previously applied to describe elastic nucleon-nucleon scattering, is extended to study η production in NN collisions. The transition amplitudes for the elementary $BN \rightarrow \eta N$ processes with B being the meson exchanged ($B = \pi, \sigma, \eta, \rho, \omega$ and δ) are taken to be the sum of four terms corresponding to s and u-channels with a nucleon or a nucleon isobar N^* (1535 MeV) in the intermediate states. Taking the relative phases of the various exchange amplitudes to be +1, the model reproduces the cross sections for the $NN \rightarrow X\eta$ reactions in a consistent manner. In the limit where all η 's are produced via N^* excitations, interference terms between the overall contribution from the exchange of pseudoscalar and scalar mesons with that of vector mesons cancel out. Consequently, much of the ambiguities in the model predictions due to unknown relative phases of different vector and pseudoscalar exchanges are strongly reduced.

1 Introduction

Much interest, both experimental[1-10] and theoretical[11-26], was devoted in recent years to the production of η meson in hadronic collisions and electroproduction processes. In analogy with π production through excitations of the Δ (1232 MeV) P33 resonance, it is believed that η -meson production in nucleon-nucleon (NN) collisions proceeds via the excitation of nucleon isobars. Because of isospin conservation however, only $I=\frac{1}{2}$ N^* isobars which decay into ηN pair are important. Pion and photon induced reactions[9, 27] provide strong evidence that near threshold, the $N^*(1535$ MeV) S_{11} resonance dominates η production. This is not unexpected in view of the proximity of its mass to that of the ηN pair and, its large branching ratio (30-55%) for $N^* \rightarrow \eta N$ decay[28]. The couplings to other resonances are weak and seem to play a minor role close to threshold.

The production of η mesons in NN collisions was considered by several groups[11-16] within one boson exchange (OBE) models, where the N^* (1535 MeV) is excited via the exchange of a boson B and then decays into ηN pair. Much of the uncertainties in the predictions of these model calculations concern the coupling of the mesons exchanged to the S11 resonance. The coupling of the π and η are known from the decay widths of this resonance but not so well the coupling of other mesons. Assuming vector meson dominance, Germond and Wilkin[12] determined the ρ coupling from $\gamma N \rightarrow N^*$ data and, as there is no evidence for isoscalar photon coupling to the N^* they neglect the contribution from ω exchange. Vetter et al.[14] determined the ρ coupling from the empirical decay width of 5% for the N^* to decay into two pions. They suggested a value $g_{\rho NN^*} = 0.615$, nearly a factor of ≈ 2.7 weaker than that deduced by Germond and Wilkin[12]. Although no experimental evidence exists, they assumed that the ω also couples to the N^* with $g_{\omega NN^*} = 0.436$, resulting with about equal ρ and ω contributions[14]. Contrary to this, with the ρ coupling taken from vector dominance, the cross section is dominated by ρ exchange[16] while the ω with a coupling as proposed by Vetter et al.[14] may influence the total cross section at most by $\approx 30 - 40\%$. It is not clear though whether such a contribution is required to explain the existing $pp \rightarrow pp\eta$ data.

In addition to these uncertainties concerning the coupling constants, the relative phases of different meson exchange amplitudes are unknown. Taking these to be ones of signs and restricting the model to π , η , ω and ρ exchanges only, there are eight solutions for the transition amplitude, one for each of the sign combinations possible. A solution, where the ρ and π exchanges add destructively, seems to explain best the cross section data for the $pp \rightarrow pp\eta$ reaction[12, 13, 16].

It is the aim of the present work to consider η meson production in NN collisions within a relativistic covariant OBE model, where a virtual boson B produced on one of the incoming nucleons, is converted into an η meson on the second nucleon (see Fig. 1). Each of the different exchange contributions to the production amplitude is determined by three factors, representing a source function of the B-N-N vertex, a boson propagator and a conversion amplitude for the $BN \rightarrow \eta N$ process. Only the latter depends on unknown boson-isobar couplings.

In variation with previous calculations the η production amplitude includes four terms, corresponding to s and u- channels with nucleon isobars (diagram 2a-2b) and nucleon excitations (diagram 2c-2d) in the intermediate states. At threshold the contribution from s-channel N^* pole (diagram 2c), hereinafter referred to as a resonance production term, dominates the process. The other diagrams, by far less important, furnish a background term. Though the various exchange amplitudes and calculated cross sections remain similar to the ones calculated previously using a non relativistic OBE model[16], the present model has distinct features which make predictions considerably more reliable. Particularly, in the limit where all η 's are produced via N^* excitations, interference terms between the overall contribution from scalar and pseudoscalar meson exchanges with that from vector mesons cancel out. Consequently, the model predictions are insensitive to the choice of the relative phases of vector meson exchanges with respect to those of scalar and pseudoscalar mesons.

The paper is organized as follows. In Sect. 2 details of the formalism and model parameters are presented. In Sect. 3 we write the S-wave production amplitude in a simple form suitable for numerical calculations. In Sect. 4 we discuss interference between various exchange contributions. The relative importance of various contributions to the amplitude and cross section for the $NN \rightarrow NN\eta$ reactions is studied

in Sect. 5. At energies close to threshold, final state interactions (FSI) strongly influence the scale and energy dependence of the calculated cross sections[15, 16]. These are introduced in Sect. 6 where comparison with data is to be made. We conclude and summarize in Sect. 7.

2 Formalism

To calculate the primary production amplitude for the $NN \rightarrow X\eta$ reactions, with X designating a bound or unbound two-nucleon state, we employ a fully covariant formalism based on an effective OBE model. We assume a reaction mechanism as depicted in Fig. 2, where a boson B created on one of the incoming nucleons is converted into an η meson on the second one via a conversion process, $BN \rightarrow \eta N$. We include both nucleon and N^* (1535 MeV) isobar excitations in the intermediate states. We do not include diagrams in which the η is produced on an internal meson line. Because of isospin and parity conservation only diagrams with σ and δ lines may contribute, but these are expected to be negligible small due to the weak coupling constants involved.

2.1 Lagrangian

The effective Lagrangian density is taken as,

$$\begin{aligned}
L = & \frac{f_{\pi NN}}{m_\pi} \bar{N} \gamma^5 \gamma^\mu \partial_\mu \vec{\pi} \vec{\tau} N + \frac{f_{\eta NN}}{m_\eta} \bar{N} \gamma^5 \gamma^\mu \partial_\mu \eta N + g_{\sigma NN} \bar{N} \sigma N + \\
& g_{\delta NN} \bar{N} \vec{\tau} \vec{\delta} N + \bar{N} [g_{\rho NN} \gamma^\mu + \frac{f_{\rho NN}}{2M} \sigma^{\mu\nu} \partial_\nu] \vec{\tau} \vec{\rho}_\mu N + g_{\omega NN} \bar{N} \gamma^\mu \omega_\mu N + \\
& [g_{\pi NN^*} \bar{N}^* \vec{\tau} \vec{\pi} N + g_{\eta NN^*} \bar{N}^* \eta N + i g_{\sigma NN^*} \bar{N}^* \gamma^5 \sigma N + \\
& g_{\rho NN^*} \bar{N}^* \gamma^5 \gamma^\mu \vec{\tau} \vec{\rho}_\mu N + g_{\omega NN^*} \bar{N}^* \gamma^5 \gamma^\mu \omega_\mu N + i g_{\delta NN^*} \bar{N}^* \gamma^5 \delta N + h.c.] , \quad (1)
\end{aligned}$$

where N , N^* , π , σ , η , ρ , ω and δ represent the fields of a nucleon, a nucleon isobar and the mesons in the spin isospin space; M and m_B are the mass of the nucleon and a meson B ; $\vec{\tau}$ are Pauli matrices acting in the isospin space and the γ 's denote Dirac matrices. This is a simple generalization of a Lagrangian used by Machleidt et al.[29] to describe NN elastic scattering data. As in Ref.[29] a pseudovector coupling is assumed for the πNN and ηNN vertices and the ωNN tensor coupling $f_{\omega NN}$ is set to

be zero. It is to be noted that using pseudoscalar couplings rather than pseudovector couplings for the π and η mesons would not alter the principal conclusions from the present work. But, taking the ω tensor coupling to be zero has the consequence that the ω exchange contribution to η production rate via N^* excitations vanishes for the $pp \rightarrow pp\eta$ reaction (see Sect. 3).

Note also that the interaction Lagrangian densities for the σ and δ mesons in Eqn. 1 are chosen in the form $ig_{BNN^*}[\bar{N}^*\gamma^5NB + \bar{N}\gamma^5N^*B]$. As we show in Appendix A, the coupling constants g_{BNN^*} ($B = \sigma, \delta$) are related through an effective triangle diagram, to g_{BNN} , $g_{\pi NN}$ and $g_{\pi NN^*}$, and this form ascertains that all of these quantities be real numbers.

2.2 The primary production amplitudes

Suppose now that the production of a pseudoscalar meson $NN \rightarrow NN P$ reaction proceeds via the mechanism depicted in Fig. 1. The primary production amplitude can then be written in the form,

$$M_{if}^{in} = \sum_B [T_{BN \rightarrow PN}(p_4, k; p_2, q)G_B(q)S_{BNN}(p_3, p_1)] + [1 \leftrightarrow 2; 3 \leftrightarrow 4], \quad (2)$$

where $S_{BNN}(p_3, p_1)$ and $G_B(q)$ represent the source function and propagator of the boson B, and $T_{BN \rightarrow PN}$ being the amplitude for the $BN \rightarrow PN$ transition. For the reactions to be considered, the latter depends on the unknown couplings to the nucleon isobar. The parameterization of the source functions and boson propagators is rather well determined from fitting NN elastic scattering data. In Eqn. 2 p_i, q and k designate 4-momenta for the i-th nucleon, the boson exchanged (B) and the meson produced (P). The sum runs over all possible boson exchanges which contribute to the process. The bracket $[1 \leftrightarrow 2; 3 \leftrightarrow 4]$ stands for a similar sum with the momenta p_1, p_3 and p_2, p_4 being interchanged.

To make the present paper reasonably self contained we write in what follows the expressions for the source functions, propagators and conversion amplitudes. We use covariant parameterizations for S_{BNN} and $T_{BN \rightarrow PN}$. For scalar and pseudoscalar mesons the propagator and source function are[30, 31],

$$G_{S,P}(q^2) = i/(q^2 - m_B^2 + i\epsilon), \quad (3)$$

$$S_{NN} = \bar{u}(p_3) I u(p_1) F_S(q^2) , \quad (4)$$

$$S_{PN} = \bar{u}(p_3) \gamma^5 I u(p_1) F_P(q^2) , \quad (5)$$

where $F_B(q^2)$ is a source form factor and I the appropriate isospin operator, i.e., $I = 1$ and $I = \vec{\tau}$ for isoscalar and isovector mesons, respectively. Here u is a nucleon Dirac spinor and $p_3 = p_1 - q$ is the final nucleon momentum (see Fig. 1). The Dirac spinors as well as the amplitudes $T_{BN \rightarrow NN}$ and M_{if}^{in} are normalized as in Itzykson and Zuber[31].

Without making unnecessary limiting assumptions about the reaction mechanism, the amplitude for the conversion process of a scalar into a pseudoscalar meson , $SN \rightarrow PN$, has the usual form [30],

$$T_{SN \rightarrow PN}(p_4, k; p_2, q) = \bar{u}(p_4) \gamma^5 [A_S + \frac{\not{k} + \not{q}}{2} B_S] I u(p_2) . \quad (6)$$

Similarly, the amplitude for the conversion of a pseudoscalar meson into another pseudoscalar meson, $P_1N \rightarrow P_2N$, is given by,

$$T_{P_1N \rightarrow P_2N}(p_4, k; p_2, q) = \bar{u}(p_4) [A_P + \frac{1}{2}(\not{k} + \not{q}) B_P] I u(p_2) . \quad (7)$$

Here $\not{q} = \gamma^\mu a_\mu$ and the quantities $A_{S(P)}$, $B_{S(P)}$ are invariant functions depending on the Mandelstam variables. These functions have an isospin structure in accordance with the following rules :

- i) $A_S = A \times 1$ for both B and P being isoscalar particles;
- ii) $A_S = A \times \vec{\tau}$ for B being isovector and P isoscalar or vice versa;
- iii) $A_S^{ab} = A^0 \times \delta^{ab} + A^1 \times [\tau^a, \tau^b]$ for B and P being both isovector particles. In Subsection. 2.3 we shall calculate these functions for the model proposed using the effective interaction Lagrangian, Eqn. 1.

The propagator for a vector meson is defined as,

$$G_{\mu\nu}^V = -i \frac{g_{\mu\nu} - q_\mu q_\nu / m^2}{q^2 - m_B^2 + i\epsilon} , \quad (8)$$

where $g_{\mu\nu}$ is the metric tensor. Generally, a vector source is the sum of vector and tensor current terms,

$$S_{VNN}^\mu(p_1, p_3) = \bar{u}(p_3) [\gamma^\mu F_V^{(1)}(q^2) + i\sigma^{\mu\nu} q_\nu F_V^{(2)}(q^2)] I u(p_1) , \quad (9)$$

with $F_V^{(1)}(q^2)$ and $F_V^{(2)}(q^2)$ standing for vector and tensor source form factors, quantities being the analogous of the nucleon electromagnetic form factors. This last expression contains conserved currents only and therefore satisfies current conservation, *i.e.*,

$$q_\mu S_V^\mu NN(q) = 0 . \quad (10)$$

Likewise, the conversion amplitude of a vector meson into a pseudoscalar meson, $VN \rightarrow PN$, is expressed in terms of eight invariant functions $A_{V,i}$ ($i = 1 - 8$) all having an isospin structure as mentioned above for the A_S and B_S . More concisely we write,

$$T_{VN \rightarrow PN}^\mu(p_4, k; p_2, q) = \bar{u}(p_4)\gamma^5[\gamma^\mu A_{12}^V + p_4^\mu A_{34}^V + k^\mu A_{56}^V + q^\mu A_{78}^V]Iu(p_2) , \quad (11)$$

where $A_{ij}^V = A_{V,i} - \not{k}A_{V,j}$. It is worth noting that because of current conservation, Eqn. 10, only the first term of Eqn. 8 may contribute to the production process so that,

$$G_{\mu\nu}^V S_{VNN}^\nu \equiv \frac{-ig_{\mu\nu}}{q^2 - m_B^2 + i\epsilon} S_{VNN}^\nu . \quad (12)$$

Also, for this same reason, the term $q^\mu A_{78}^V$ in Eqn. 11 does not contribute to the production amplitude, $M^{(in)}$. By using straightforward algebra of γ matrices and the Dirac equation for a free particle and, by substituting equivalent two-component free spinor matrix elements (Table A6.1 of Ref. [32]) in Eqns. 3-11 we may write the primary production amplitude as,

$$M_{NN \rightarrow PNN}^{in}(p_1, p_2; p_3, p_4, k) = \sum_S M_S^{in} + \sum_P M_P^{in} + \sum_V M_V^{in} + [1 \leftrightarrow 2; 3 \leftrightarrow 4], \quad (13)$$

where the sums over S, P, and V run, respectively, over all scalar, pseudoscalar and vector mesons and,

$$M_S^{in} = S_0 + S_{13}^k \sigma_{13}^k + \tilde{S}_{24}^k \sigma_{24}^k + S^{kl} \sigma_{13}^k \sigma_{24}^l , \quad (14)$$

$$M_P^{in} = P_{13}^k \sigma_{13}^k + P^{kl} \sigma_{13}^k \sigma_{24}^l , \quad (15)$$

$$M_V^{in} = V_0 + V_{13}^k \sigma_{13}^k + \tilde{V}_{24}^k \sigma_{24}^k + V^{kl} \sigma_{13}^k \sigma_{24}^l . \quad (16)$$

In Eqns. 14-16 all of the quantities $S_0, V_0; S_{ij}, P_{ij}, V_{ij}; \tilde{S}_{ij}, \tilde{V}_{ij}; S^{nm}, P^{nm}, V^{nm}$ are functions of the particle momenta involved. Their definitions are given in Appendix B for the general case in terms of the invariant functions.

2.3 The invariant functions

To complete the derivation of the η production amplitude the invariant functions A and B must be specified. To do this we assume that the conversion process proceeds via the mechanisms of Fig. 3, and consider as an example the transition amplitude for the $\omega N \rightarrow \eta N$ process. Using the usual Feynman rules and vertices of the Lagrangian, Eqn. 1, one writes,

$$T_{\omega p \rightarrow \eta p}^\mu = -iu(p_4) \{ g_{\omega NN^*} g_{\eta NN^*} \gamma^\mu \gamma^5 [G_R(s_{13}) + G_R(u_{13})] + g_{\omega NN} \frac{f_{\eta NN}}{m_\eta} [k^\mu \gamma^\mu \gamma^5 G_N(s_{13}) - \gamma^5 (k_\mu - i\sigma^{\mu\nu} k_\nu) G_N(u_{13})] \} u(p_2) , \quad (17)$$

where $s_{13} = (k + p_4)^2$, $u_{13} = (p_2 - k)^2$ and G_N denotes a nucleon propagator

$$G_N = \frac{i}{\not{p} - M + i\epsilon} . \quad (18)$$

For an isobar the mass in Eqn. 18 is replaced by a mass operator, *i.e.*,

$$G_R = \frac{i}{\not{p} - M_R + i\Gamma_R/2} . \quad (19)$$

Generally speaking, M_R and Γ_R are the real and imaginary parts of the isobar self energy, quantities representing the mass and width of the resonance. Both of these are functions of the Mandelstam variable $s = p^2$. It is straightforward to show that at resonance, where $\sqrt{s} \approx M_R$, Eqn. 19 simplifies to the usual Breit-Wigner form,

$$G_R(s) = \frac{-i}{M_R - \sqrt{s} - i\Gamma_R/2} . \quad (20)$$

For future use we define two related quantities,

$$\Delta_N(x) = i/(x - M^2 + i\epsilon) , \quad (21)$$

and

$$\Delta_R(x) = -i/(M_R - \sqrt{x} - i\Gamma_R/2) . \quad (22)$$

Altogether there are four terms in Eqn. 17 corresponding to s and u-channels with N^* (diagrams 3a-3b) and with nucleon (diagrams 3c-3d) poles. By comparing Eqn. 17 with Eqn. 11 one obtains,

$$A_{\omega,1} = g_{\omega NN^*} g_{\eta NN^*} \tilde{G}_R + ig_{\omega NN} \frac{f_{\eta NN}}{m_\eta} X_V , \quad (23)$$

$$A_{\omega,2} = -2iMg_{\omega NN} \frac{f_{\eta NN}}{m_\eta} \tilde{G}_N , \quad (24)$$

$$A_{\omega,5} = i2Mg_{\omega NN} \frac{f_{\eta NN}}{m_\eta} \Delta_N(s_{13}) , \quad (25)$$

$$A_{\omega,3} = A_{\omega,4} = A_{\omega,6} = A_{\omega,7} = A_{\omega,8} = 0 . \quad (26)$$

Similar calculations for other meson exchanges give the following:

$$A_\sigma = g_{\sigma NN^*} g_{\eta NN^*} \tilde{G}_R - ig_{\sigma NN} \frac{f_{\eta NN}}{m_\eta} X_S , \quad (27)$$

$$B_\sigma = i2Mg_{\sigma NN} \frac{f_{\eta NN}}{m_\eta} \tilde{G}_N , \quad (28)$$

$$A_\delta = g_{\delta NN^*} g_{\eta NN^*} \tilde{G}_R \vec{\tau} - ig_{\delta NN} \frac{f_{\eta NN}}{m_\eta} X_S \vec{\tau} , \quad (29)$$

$$B_\delta = i2Mg_{\delta NN} \frac{f_{\eta NN}}{m_\eta} \tilde{G}_N \vec{\tau} , \quad (30)$$

$$A_\pi = g_{\pi NN^*} g_{\eta NN^*} \tilde{G}_R \vec{\tau} , \quad (31)$$

$$B_\pi = -\frac{f_{\eta NN}}{m_\eta} \frac{f_{\pi NN}}{m_\pi} X_P \vec{\tau} , \quad (32)$$

$$A_\eta = g_{\eta NN^*}^2 \tilde{G}_R , \quad (33)$$

$$B_\eta = -\frac{f_{\eta NN}^2}{m_\eta^2} X_P , \quad (34)$$

$$A_{\rho,1} = g_{\rho NN^*} g_{\eta NN^*} \tilde{G}_R \vec{\tau} + ig_{\rho NN} \frac{f_{\eta NN}}{m_\eta} X_V \vec{\tau} , \quad (35)$$

$$A_{\rho,2} = -2iMg_{\rho NN} \frac{f_{\eta NN}}{m_\eta} Y_V \vec{\tau} , \quad (36)$$

$$A_{\rho,3} = -ig_{\rho NN} \frac{f_{\eta NN}}{m_\eta} \frac{\kappa}{2M} Z_V \vec{\tau} , \quad (37)$$

$$A_{\rho,4} = -2ig_{\rho NN} \frac{f_{\eta NN}}{m_\eta} \kappa \tilde{G}_N \vec{\tau} , \quad (38)$$

$$A_{\rho,5} = i2Mg_{\rho NN} \frac{f_{\eta NN}}{m_\eta} (1 + 2\kappa) \Delta_N(s_{13}) \vec{\tau} , \quad (39)$$

$$A_{\rho,6} = -2ig_{\rho NN} \frac{f_{\eta NN}}{m_\eta} \kappa \Delta_N(s_{13}) \vec{\tau} . \quad (40)$$

In Eqns. 23 - 40 we use the notations,

$$\tilde{G}_R = \Delta_R(s_{13}) + \Delta_R(u_{13}) , \quad (41)$$

$$\tilde{G}_N = \Delta_N(s_{13}) + \Delta_N(u_{13}) , \quad (42)$$

$$X_S = (2p_2 k + m_\eta^2 - 2M^2) \Delta_N(s_{13}) + (m_\eta^2 - 2p_1 k - 2M^2) \Delta_N(u_{13}) , \quad (43)$$

$$X_P = (2p_2k + m_\eta^2 + 4M^2)\Delta_N(s_{13}) + (m_\eta^2 - 2p_1k + 4M^2)\Delta_N(u_{13}) , \quad (44)$$

$$X_V = (2p_2k + m_\eta^2)\Delta_N(s_{13}) + (2p_1k + m_\eta^2)\Delta_N(u_{13}) , \quad (45)$$

$$Y_V = (1 + \kappa + \frac{\kappa}{4M^2}(2p_2k + m_\eta^2))\Delta_N(s_{13}) + \\ (1 + \kappa + \frac{\kappa}{4M^2}(2p_1k - m_\eta^2))\Delta_N(u_{13}) , \quad (46)$$

$$Z_V = (2p_2 \cdot k + m_\eta^2)\Delta_N(s_{13}) - (2p_1 \cdot k - m_\eta^2)\Delta_N(u_{13}) . \quad (47)$$

2.4 The model parameters

In the calculations to be presented below all of the meson-nucleon-nucleon couplings are taken from Machleidt et al.[29]; their relativistic OBEP set with pseudovector coupling for the pseudoscalar mesons. For the sake of completeness these are included in Table 1. As in Ref.[29] the source form factors are taken to be,

$$F_\sigma = g_{\sigma NN}f_\sigma , \quad F_\pi = ig_{\pi NN}f_\pi , \quad F_\eta = ig_{\eta NN}f_\eta , \quad F_\delta = g_{\delta NN}f_\delta \\ F_\rho^{(1)} = g_{\rho NN}f_\rho , \quad F_\rho^{(2)} = \frac{\kappa}{2M}g_{\rho NN}f_\rho , \quad F_\omega^{(1)} = g_{\omega NN}f_\omega ,$$

with the parameterization,

$$f_B(q^2) = \frac{\Lambda_B^2 - m_B^2}{\Lambda_B^2 - q^2} . \quad (48)$$

The π and η couplings to the N^* (1535 MeV) are deduced from the partial widths of the N^* to decay into πN and ηN ; their values are rather well accepted (see Refs. [12-16]). The $g_{\rho NN^*}$ is deduced from $\gamma N \rightarrow N^*$ data and vector dominance[12]. For the other mesons there exists no direct information which can be used to determine their coupling to the N^* . In Ref.[14] the ω coupling is evaluated from the relation,

$$\frac{g_{\omega NN^*}}{g_{\omega NN}} = \frac{g_{\pi NN^*}}{g_{\pi NN}} . \quad (49)$$

Assuming SU(3) flavor symmetry it can be shown also that,

$$\frac{g_{\omega NN^*}}{g_{\omega NN}} = \frac{g_{\rho NN^*}}{g_{\rho NN}(1 + \kappa_\rho)} . \quad (50)$$

Taking the appropriate constants from Table 1 one obtains $g_{\omega NN^*} \approx 1$ from both of these expressions. This is a factor of two higher than that suggested by Vetter et al.[14]. Similarly, from using effective triangle diagrams (see Appendix A) the $g_{\sigma NN^*}$ and $g_{\delta NN^*}$ are also related to the pion constants through an expression similar to Eqn. 49.

3 Amplitudes and cross sections

In this section we write S-wave production amplitudes for the $pp \rightarrow pp\eta$ and $pn \rightarrow pn\eta$ reactions in a simple form which is suitable for numerical calculations. To this aim let us call,

$$\Pi_j = \frac{\mathbf{p}_j}{\sqrt{E_j + M}} , \quad (51)$$

where \mathbf{p}_j and E_j are three-momentum and total energy of the j-th nucleon. For the incoming particles in the CM system, $\Pi_1 = -\Pi_2 = \Pi$. The total energy square is $s = (p_1 + p_2)^2$. Then the energy available in the CM system is,

$$Q = \sqrt{s} - 2M - m_\eta . \quad (52)$$

We shall calculate the amplitudes and cross sections as functions of Q .

There are two amplitudes one isovector M_{11} and one isoscalar M_{00} which determine completely the cross sections for the $NN \rightarrow X\eta$ reactions at rest. These two amplitudes correspond to the $^{33}P_0 \rightarrow ^{31}S_0$ and $^{11}P_1 \rightarrow ^{31}S_1$ transitions in the two-nucleon system. Only M_{11} contributes to the rate of the $pp \rightarrow pp\eta$ reaction. Likewise only M_{00} contributes to the $np \rightarrow d\eta$ reaction, but both amplitudes contribute to the rate of the $np \rightarrow np\eta$ reaction. Following the discussion in subsection 2.2 we write these amplitudes as,

$$M_{11} = M_\pi + M_\eta + M_\sigma + M_\delta + M_\rho + M_\omega , \quad (53)$$

$$M_{00} = -3M_\pi + M_\eta + M_\sigma - 3M_\delta - 3M_\rho + M_\omega , \quad (54)$$

where M_B stands for a partial exchange amplitude of a meson B. The factor of -3 is due to isospin. By evaluating matrix elements of the expressions, Eqns. 14-15, between the allowed initial and final spin states and substituting for the appropriate invariant functions listed in subsection 2.3, we obtain,

$$M_\sigma = iG_{\sigma NN}(g_{\sigma NN^*}g_{\eta NN^*}R + g_{\sigma NN}g_{\eta NN}\Sigma_S) , \quad (55)$$

$$M_\delta = iG_{\delta NN}(g_{\delta NN^*}g_{\eta NN^*}R + g_{\delta NN}g_{\eta NN}\Sigma_S) , \quad (56)$$

$$M_\pi = iG_{\pi NN}(g_{\pi NN^*}g_{\eta NN^*}R + g_{\pi NN}g_{\eta NN}\Sigma_P) , \quad (57)$$

$$M_\eta = iG_{\eta NN}(g_{\eta NN^*}^2R + g_{\eta NN}^2\Sigma_P) , \quad (58)$$

$$M_\rho = G_{\rho NN}[g_{\rho NN^*}g_{\eta NN^*}(w_\rho \pm 2v_\rho)R + g_{\rho NN}g_{\eta NN}(\Sigma_\rho^{(1)} + 2\Sigma_\rho^{(2)})] , \quad (59)$$

$$M_\omega = G_{\omega NN}[g_{\omega NN^*}g_{\eta NN^*}(w_\omega \pm 2v_\omega)R + g_{\omega NN}g_{\eta NN}(\Sigma_\omega^{(1)} + 2\Sigma_\omega^{(2)})] . \quad (60)$$

In Eqns. 55-60 we have used the notation,

$$G_{BNN} = g_{BNN} \frac{E+M}{M} \frac{1}{M(m_\eta + Q) + m_\pi^2} f_\sigma^2(-M[m_\eta + Q])\Pi , \quad (61)$$

$$R = \frac{1}{M_R - M - m_\eta - Q - i\Gamma/2} + \frac{1}{M_R - M + m_\eta + Q - i\Gamma/2} , \quad (62)$$

$$\Sigma_S = \frac{1}{M} \left(1 - \frac{5m_\eta}{2M - m_\eta} \right) , \quad (63)$$

$$\Sigma_P = \left(\frac{m_\eta}{2M} \right)^2 \left[1 + \frac{2(E+M)}{m_\eta} \Pi \cdot \Pi \right] \frac{1}{2M + m_\eta} . \quad (64)$$

$$\Sigma_\rho^{(1)} = i \frac{m_\eta}{4M^2} \left\{ (1 + \kappa \Pi \cdot \Pi) \left[2 - \left(1 - \frac{\kappa}{2} \right) \frac{m_\eta}{2M + m_\eta} \right] + \frac{\kappa m_\eta^2}{4M(2M + m_\eta)} \right\} , \quad (65)$$

$$\Sigma_\rho^{(2)} = i\kappa(1 + \kappa) \frac{m_\eta}{2M} \left\{ -\frac{E+M}{M} \Pi \cdot \Pi \left(1 - \frac{m_\eta}{2M + m_\eta} \right) + \frac{m_\eta^2}{4M(2M + m_\eta)} \right\} , \quad (66)$$

$$\Sigma_\omega^{(1)} = i \frac{m_\eta}{4M^2} \left(2 - \frac{m_\eta}{2M + m_\eta} \right) , \quad (67)$$

$$\Sigma_\omega^{(2)} = 0 , \quad (68)$$

$$w_V = 2 + \kappa_V \left(\frac{E+M}{2M} \right) \Pi \cdot \Pi , \quad (69)$$

$$v_V = 1 + \kappa_V \left(\frac{E+M}{2M} \right) . \quad (70)$$

$$(71)$$

The $-$ and $+$ signs in the expressions for M_ρ and M_ω refer to the $^{33}P_0 \rightarrow ^{31}S_0$ and $^{11}P_1 \rightarrow ^{13}S_1$ transitions, respectively. The expressions for other exchange amplitudes are the same for both of these transitions. Because of kinematic, the resonance terms in Eqns. 55-60 exceed by far any of the background terms. Following the definitions of w_ρ and v_ρ , the ρ exchange amplitude, Eqn. 59, has opposite signs for the two transitions but, because of the negative isospin factor the ρ contributions in M_{11} and M_{00} have equal signs. Also note that for $\kappa_\omega \equiv 0$, $w_\omega=2$ and $v_\omega=1$ causing the first term in Eqn. 60 to vanish in the case of a $^{33}P_0 \rightarrow ^{31}S_0$ transition. Thus, only small background terms may contribute to the ω exchange amplitude, and practically,

the calculated cross section for the $pp \rightarrow pp\eta$ reaction is expected to be free from ambiguities due to the ωNN^* coupling.

Finally a general formula for the invariant cross section for the $NN \rightarrow NN\eta$ reaction is written as

$$\sigma_{TT} = \frac{(2\pi)^{-5}}{128 p^* s^{3/2}} \int d\Omega_1 d\Omega_2 \frac{d\sqrt{s_{23}}}{\sqrt{s_{23}}} \lambda^{1/2}(s, m_1^2, s_{23}) \lambda^{1/2}(s_{23}, m_2^2, m_3^2) |M_{TT} Z|^2, \quad (72)$$

where M_{TT} represents the amplitudes M_{11} and M_{00} of Eqns. 53-54; the indices 1, 2 and 3 label the outgoing particles, \sqrt{s} and $\sqrt{s_{23}}$ are the total energy and partial energy of particles 2 and 3, p^* is the center of mass (CM) momentum of the incoming proton, and Z is the FSI correction factor to be specified below. The λ is the usual triangle function defined as[33]

$$\lambda(x, y, z) = x^2 + y^2 + z^2 - 2xy - 2xz - 2yz. \quad (73)$$

4 Interference terms

As indicated in the introduction, major uncertainties in previous model calculations arise from the unknown relative phases of different meson contributions. Particularly, interference terms between prominent ρ and π contributions influence strongly the scale of the cross section. The aim of the present section is to show that in the present model and in the limit where η -meson production proceeds through N^* (1535 MeV) excitations only, interference terms between the overall contribution from scalar and pseudoscalar meson exchanges and that of vector meson exchanges cancel out. To see this let us consider the contributions to the production amplitude from N^* pole terms only. By substituting the various exchange contributions, Eqns. 55-60, into Eqn. 2 one obtains,

$$\begin{aligned} M_{NN \rightarrow PNN}^{in}(p_1, p_2; p_3, p_4, k) &= g_{\eta NN^*} R \\ &[i(G_{\pi NN} g_{\pi NN^*} + G_{\eta NN} g_{\eta NN^*} + G_{\sigma NN} g_{\sigma NN^*} + G_{\delta NN} g_{\delta NN^*}) + \\ &G_{\rho NN} g_{\rho NN^*}(w_\rho \pm 2v_\rho) + G_{\omega NN} g_{\omega NN^*}(w_\omega \pm 2v_\omega)] . \end{aligned} \quad (74)$$

We notice that all of the quantities G_{BNN} , g_{BNN^*} , w_V and v_V are real so that

$$M^{(in)} M^{(in)\dagger} = |g_{\eta NN^*} R|^2$$

$$\{[G_{\pi NN}g_{\pi NN^*} + G_{\eta NN}g_{\eta NN^*} + G_{\sigma NN}g_{\sigma NN^*} + G_{\delta NN}g_{\delta NN^*}]^2 + [G_{\rho NN}g_{\rho NN^*}(w_\rho \pm 2v_\rho) + G_{\omega NN}g_{\omega NN^*}(w_\omega \pm 2v_\omega)]^2\} . \quad (75)$$

We may thus conclude that in a model where isobar mechanism dominates, in practice, the π and ρ exchange amplitudes add incoherently and their unknown relative phases should introduce no ambiguities in the model predictions. There remain of course ambiguities due to interference amongst the different vector meson exchanges or amongst the various scalar and pseudoscalar meson exchanges to be studied below in more details.

5 Predictions

We now apply the model presented in the previous sections to calculate the energy integrated cross section for the $pp \rightarrow pp\eta$ and $pn \rightarrow pn\eta$ reactions. We consider first the relative importance of various exchange contributions. To this aim we draw in Figs. 4-5 the partial exchange amplitudes, Eqns. 55-60. Most important are the ρ and π exchanges. Other contributions are small but might be influential through interference. Taking the relative phases of the different exchange amplitudes to be ones of signs, there are altogether 32 solutions, one for each of the different sign combinations. All of these solutions yield cross sections having identical energy dependence but vary in scale. The primary production amplitudes for the $pp \rightarrow pp\eta$ and $pn \rightarrow pn\eta$ reactions calculated with all of the relative phases chosen to be +1 are shown in Fig.6. As we shall see below this phase combination, hereinafter referred to as the standard solution, explains best the cross section data at energies close to threshold for the $pp \rightarrow pp\eta$, $pn \rightarrow pn\eta$. The cross sections corresponding to these amplitudes are drawn as solid lines in Figs. 7-8. The other curves in these figures represent predictions with other phase combinations, representing the lowest (dashed curve) and highest (dotted curve) cross sections obtained. At most the scale of the calculated cross sections varies by a factor of 2–3, as compared to a factor of about 20 reported for other models[16]. To examine these ambiguities in the model predictions let us consider the standard solution in some details. Consider first the $pp \rightarrow pp\eta$ reaction. Here the individual contributions from all of the scalar and pseudoscalar meson exchanges have equal signs and therefore should add constructively. In Fig.

9 we show partial cross sections accounting for scalar and pseudoscalar exchanges (dashed curve) and vector exchanges (dash-dotted curve) separately. The solid curve (labeled σ^+) gives the total cross section for the standard solution. Although the size of these partial cross sections are comparable, reversing the relative phases for both of the ρ and ω to have the opposite signs hardly influences the predictions for the total cross section (curve labeled σ^-). Indeed, interference between vector mesons and scalar or pseudoscalar exchanges involves background terms only and consequently are very small. Also, as we have indicated above the ω exchange is very weak in this case because N^* pole terms sum to zero so that the main source of ambiguities in the model predictions is due to interference amongst the scalar and pseudoscalar contributions.

We obtain similar results for the $pn \rightarrow pn\eta$ reactions. In this case contributions from both of the $^3P_0 \rightarrow ^3S_0$ and $^1P_1 \rightarrow ^1S_1$ transitions are possible and the cross section becomes an incoherent sum,

$$\sigma_{np \rightarrow np\eta} = \frac{1}{2} [\sigma_{11} + \sigma_{00}] . \quad (76)$$

The calculated cross sections are shown in Fig. 10. Again the phase between the overall contribution from vector meson exchanges with respect to the overall contribution from scalar and pseudoscalar does not affect much the calculated total cross section. In this case the process is dominated by a ρ meson exchange. The contributions from ω exchanges through N^* excitations do not cancel out (see Eqn. 60), giving rise to a relatively large ω exchange contribution, so that interference with a dominant ρ exchange amplitude determines, to a large extent, the scale of the calculated cross section. As for the $pp \rightarrow pp\eta$ reaction, in the standard solution which explains data the ρ and ω add destructively. The isovector π and δ contributions add destructively to those of the isoscalar η and σ .

6 FSI and comparison with data

At energies close to threshold FSI corrections influence the energy dependence and scale of the calculated cross section. To allow comparison with data to be made, we introduce FSI in an approximate way following the procedure of Refs. [15, 16, 34].

The S-wave transition amplitude for a three body reaction, say $NN \rightarrow NN\eta$, is assumed to factorize in the form

$$T_{if} \approx M_{if}^{in} T_{ff}^{el} , \quad (77)$$

where M_{if}^{in} stands for the primary production amplitude and T_{ff}^{el} represents the FSI correction factor. We identify this factor with the on mass-shell elastic scattering amplitude for the $NN\eta \rightarrow NN\eta$ (three particles in to three particles out transition). The validity of this approximation was discussed at length previously[34]. Here we recall only that, T_{ff}^{el} is a solution of the Faddeev's equations and has the structure of the Faddeev's decomposition of the t-matrix for $3 \rightarrow 3$ transition. It is estimated using on mass shell two-body elastic scattering amplitudes, $t_{\eta N}$ and t_{NN} , in a three-body space where the third particle being a spectator. We calculate these from S-wave phase shifts. The S-wave pp phase shift is calculated using the modified Cini-Fubini-Stanghellini (CFS) formula[35] with a proton-proton scattering length $a_{pp} = -7.82 fm$ and an effective range $r_{pp} = 2.7 fm$. Similarly, the np S-wave singlet and triplet phase shifts are calculated using the so called mixed effective range expansion with CFS shape corrections. The scattering lengths and effective ranges are taken to be $a_t = 5.413 fm$ and $r_t = 1.735 fm$ for triplet scattering and $a_s = -23.715 fm$ and $r_s = 2.73 fm$ for the singlet. The values of the CFS shape correction parameters are taken to be $p_1 = 0.1147 fm^3$ and $p_2 = 3.861 fm^2$. The $t_{\eta N}$ is taken from Ref. [23] to be

$$[t(\eta N \rightarrow \eta N)]^{-1} = 1/a + rk^2/2 - ik_{\eta} , \quad (78)$$

with ηp scattering length and effective range

$$a = (0.476 + 0.276i) fm, \quad r = (-3.16 - 0.13i) fm . \quad (79)$$

Albeit, FSI corrections modify the energy dependence of the cross section at low energy region (Q below 15 MeV) and should not influence much predictions at higher energies.

In Figs. 11-12 we draw our predictions for the energy integrated cross sections for the $pp \rightarrow pp\eta$ and $pn \rightarrow pn\eta$ reactions with FSI corrections included, along with data taken from Refs. [2-6]. The solid curve gives the standard solution, i.e., with

the relative phases of the various exchange amplitudes taken to be +1. The model explains fairly well the cross section data for both of these processes. Calculations which include resonance terms only and without background terms are drawn as dashed curves. Clearly, the η production is dominated by the $N^*(1535 \text{ MeV})$ isobar excitations (diagram 2a). The effects of the background terms (diagrams 2b-2d) are bound to 10% or less in the near threshold energy region considered here. FSI corrections for the $np \rightarrow np\eta$ reaction are performed separately for σ_{11} and σ_{00} using the appropriate singlet and triplet np S-wave phase shifts. The model reproduces the cross section data for all of the $pp \rightarrow pp\eta$, $pn \rightarrow pn\eta$ and $pn \rightarrow d\eta$ reactions. The results for the latter process will be reported elsewhere[36].

As indicated in the introduction, there exists no direct evidence for the coupling of the σ , δ and ω mesons to the $N^*(1535 \text{ MeV})$ isobar. It is interesting to see whether contributions from these mesons are required to explain data. To this aim, calculations were repeated with : (i) $g_{\omega NN^*} = 0$, (ii) $g_{\omega NN^*} = g_{\sigma NN^*} = 0$, (iii) $g_{\omega NN^*} = g_{\sigma NN^*} = g_{\delta NN^*} = 0$. The predictions with $g_{\omega NN^*} = 0$ are shown in Figs. 11-12 as dot-dashed curves. They explain equally well the data for the $pp \rightarrow pp\eta$ reaction, and for the $pn \rightarrow pn\eta$ reaction the agreement is even slightly better. The effects of the σ and δ are negligibly small and their contributions seem not to be needed either (see Figs. 12-13).

7 Summary and Discussion

In this paper we have presented a covariant OBE model for η production in NN collisions. The model includes nucleon and $N^*(1535 \text{ MeV})$ isobar excitations in the intermediate states and contributions from all of the $\pi, \eta, \sigma, \rho, \omega$ and δ meson exchanges. Our starting point was a Lagrangian which describes NN scattering, in a consistent manner, in terms of these same meson exchanges.

As in other similar calculations, the model predictions are subject to uncertainties due to the unknown relative phases of the various exchange amplitudes, but these are now limited to only a factor of 2-3 in the calculated cross sections. The present formalism allows a thorough discussion of interference between the various contributions. We have shown that interference effects between vector and scalar or

pseudoscalar meson exchanges are negligibly small. Bearing in mind that the most prominent contributions are those due to the π and ρ exchanges this feature of the model renders predictions to be considerably more reliable than our previous model calculations[16]. Assuming that the relative phases of all of the various exchange amplitudes to be +1, the model reproduces the cross section data, both the scale and energy dependence, for the $pp \rightarrow pp\eta$ and $pn \rightarrow pn\eta$ reactions. As indicated above the model also reproduces the cross section data for the $np \rightarrow d\eta$ reaction[36]

The ω , σ and δ contributions are small and with the present accuracies of the measurements seem unnecessary to explain the data. This is not unwarranted property of the model since there is no direct evidence for the coupling of these mesons to the N^* (1535 MeV) isobar. Finally, with the ρ coupling lowered to $g_{\rho NN^*} = 0.615$, as low as suggested by Vetter et al.[14], no solution is found which explains data simultaneously for all of the $NN \rightarrow X\eta$ reactions. It would be interesting to determine this coupling anew.

Acknowledgments This work was supported in part by the Israel Ministry Of Absorption. We are indebted to Z. Melamed for assistance in computation.

8 Appendix A

In this Appendix we describe the derivation of the expressions used to calculate $g_{\sigma NN^*}$ and $g_{\delta NN^*}$ (see caption of Table 1). Consider the effective triangle diagram of Fig. 14 and take the $\sigma\pi\pi$ vertex to have the general form,

$$V_{\sigma\pi\pi} = g_{\sigma\pi\pi} v_{\sigma\pi\pi}(k, q - k, q) . \quad (80)$$

For a Lagrangian density, $L_{int} = g_{\sigma\pi\pi} M \sigma \vec{\pi} \cdot \vec{\pi}$, the function $v_{\sigma\pi\pi}(k, q - k, q)$ becomes,

$$v_{\sigma\pi\pi}(k, q - k, q) = M f_1(k^2, q^2) , \quad (81)$$

where $f_1(k^2, q^2)$ is a scalar function. Taking the Lagrangian density to be, $L_{int} = (g_{\sigma\pi\pi}/M)(\sigma \partial \vec{\pi}) \cdot (\partial \vec{\pi})$, yields,

$$v_{\sigma\pi\pi}(k, q - k, q) = \frac{1}{M}(q - k) q f_2(k^2, q^2) . \quad (82)$$

As will be demonstrated below the actual form of $v_{\sigma\pi\pi}$ does not influence the final results for the calculated coupling constants. Suppose now that one of the nucleon is on mass shell, *i.e.*, $p^2 = M^2$, then using the loop diagram Fig. 14 the σNN coupling is[37],

$$g_{\sigma NN} v_{\sigma NN}(k, p - k, p) = -i \frac{g_{\sigma\pi\pi} g_{\pi NN}^2}{(2\pi)^4} \int d^4 q \not{q} v_{\sigma\pi\pi}(k, q - k, q) \left\{ (q^2 - m_\pi^2)[(q - k)^2 - m_\pi^2][(p - q)^2 - M^2] \right\}^{-1} . \quad (83)$$

By using the standard Feynman parameterization and shift of the integration variable one obtains,

$$g_{\sigma NN} v_{\sigma NN}(k, p - k, p) = g_{\sigma\pi\pi} g_{\pi NN}^2 [\not{p} X(k, p - k, p) + \not{k} Y(k, p - k, p)] , \quad (84)$$

where,

$$X(k, p - k, p) = 2 \int dx_1 dx_2 dx_3 x_3 \delta(1 - x_1 - x_2 - x_3) I_q , \quad (85)$$

$$Y(k, p - k, p) = 2 \int dx_1 dx_2 dx_3 x_2 \delta(1 - x_1 - x_2 - x_3) I_q , \quad (86)$$

and I_q is the usual integral over the Euclidean four-vector \tilde{q} [31],

$$I_q = \frac{1}{(2\pi)^4} \int d^4 \tilde{q} v_{\sigma\pi\pi}(k, q + p x_3 + k[x_2 - 1], q + p x_3 + k x_2) \left[(\tilde{q}^2 - (q + p x_3 + k x_2)^2 + k^2 x_2 + m_\pi^2 (x_1 + x_3)) \right]^{-3} . \quad (87)$$

To evaluate the $g_{\sigma NN^*}$ coupling constant we have to replace one of the two πNN vertices with a πNN^* vertex. This leads to,

$$g_{\sigma NN^*} v_{\sigma NN^*}(k, p - k, p) = g_{\sigma\pi\pi} g_{\pi NN} g_{\pi NN^*} [\not{p}X(k, p - k, p) + \not{k}Y(k, p - k, p)] . \quad (88)$$

After some algebra,

$$g_{\sigma NN} v_{\sigma NN}(k, p - k, p) = g_{\sigma\pi\pi} g_{\pi NN}^2 J , \quad (89)$$

$$g_{\sigma NN^*} v_{\sigma NN^*}(k, p - k, p) = g_{\sigma\pi\pi} g_{\pi NN} g_{\pi NN^*} J , \quad (90)$$

with,

$$J = [M^2 X^2 + k^2 Y^2 + 2pkXY]^{1/2} . \quad (91)$$

From Eqns. 89 and 90, one sees that the functions $v_{\sigma NN}$ and $v_{\sigma NN^*}$ are identical up to a scale factor, which we may absorb into the constant $g_{\sigma NN^*}$. Thus, Eqns. 89 and 90 are equivalent to,

$$\frac{g_{\sigma NN^*}}{g_{\sigma NN}} = \frac{g_{\pi NN^*}}{g_{\pi NN}} \quad (92)$$

Note that taking the σ coupling to be $ig_{\sigma NN^*}[\bar{N}^* \gamma^5 N + \bar{N} \gamma^5 N^*]$, as in Eqn. 1, lead to a real $g_{\sigma NN^*}$. Otherwise with this coupling taken as $g_{\sigma NN^*}[\bar{N}^* \gamma^5 N - \bar{N} \gamma^5 N^*]$, one obtains a pure imaginary $g_{\sigma NN^*}$.

Similar calculations can be made for the $g_{\delta NN^*}$ leading to a similar expression, *viz*,

$$\frac{g_{\delta NN^*}}{g_{\delta NN}} = \frac{1}{2} \left[\frac{g_{\pi NN^*}}{g_{\pi NN}} + \frac{g_{\eta NN^*}}{g_{\eta NN}} \right] . \quad (93)$$

9 Appendix B

In what follows we write explicit expressions for the vectors and tensors of Eqns. 14-16. Let i, j label the i -th and j -th nucleon (see Fig. 1). We define,

$$\phi_{ij}^{\pm} = 1 \pm \Pi_i \cdot \Pi_j , \quad (94)$$

$$\Sigma_{ij} = \Pi_i + \Pi_j , \quad (95)$$

$$\Delta_{ij} = \Pi_i - \Pi_j , \quad (96)$$

$$\chi_{ij} = \Pi_i \times \Pi_j . \quad (97)$$

Then for a scalar meson exchange,

$$S_0 = iF_S(q^2)G_S(q^2)T_S^{(1)} , \quad (98)$$

$$S_{13}^l = F_S(q^2)G_S(q^2)T_S^{(1)}\chi_{13}^l , \quad (99)$$

$$\tilde{S}_{24}^l = F_S(q^2)G_S(q^2)\phi_{13}^-T_S^{(2)} , \quad (100)$$

$$S^{kl} = iF_S(q^2)G_S(q^2)\chi_{13}^kT_S^{(2)l} , \quad (101)$$

with,

$$T_S^{(1)} = \frac{1}{2}(\mathbf{k} + \mathbf{q}) \cdot \chi_{13}B_S , \quad (102)$$

$$T_S^{(2)} = A_S\Delta_{24}^l + \frac{1}{2}B_S[(\mathbf{k} + \mathbf{q}) \cdot \Pi_4\Pi_2^l + (\mathbf{k} + \mathbf{q}) \cdot \Pi_2\Pi_4^l + \phi_{24}^-(\mathbf{k} + \mathbf{q})^l - (k_0 + q_0)\Sigma_{24}^l] . \quad (103)$$

For a pseudoscalar exchange,

$$P_{13}^l = G_P(q^2)F_P(q^2)T_P^{(1)}\Delta_{13}^l ,$$

$$P^{kl} = iF_P(q^2)G_P(q^2)\Delta_{13}^kT_S^{(2)l} , \quad (104)$$

with,

$$T_P^{(1)} = A_P\phi_{24}^- + \frac{1}{2}B_S[\phi_{24}^+(k_0 + q_0) + (\mathbf{k} + \mathbf{q}) \cdot \Sigma_{24}] ,$$

$$T_P^{(2)l} = A_P\chi_{24}^l - \frac{1}{2}B_S[(k_0 + q_0)\chi_{24}^l + (\mathbf{k} + \mathbf{q}) \times \Delta_{24}^l] . \quad (105)$$

For a vector meson exchange,

$$V_0 = iG_V(q^2)C_{13}^\mu X_{24,\mu} ,$$

$$V_{13}^l = -G_V(q^2)D_{13}^{\mu l} X_{24,\mu} ,$$

$$\tilde{V}_{24}^l = G_V(q^2)C_{13}^{\mu l} Y_{24,\mu}^l ,$$

$$V^{ln} = iG_V(q^2)D_{13}^{\mu l} Y_{24,\mu}^n , \quad (106)$$

where,

$$C_{13}^0 = F_V^{(1)}\phi_{24}^+ + F_V^{(2)}\mathbf{q} \cdot \Delta_{13} , \quad (107)$$

$$C_{13}^m = F_V^{(1)}\Sigma_{24}^m + F_V^{(2)}(q^0\Delta_{13}^m - \Pi_1^m\mathbf{q} \cdot \Pi_3 - \Pi_3^m\mathbf{q} \cdot \Pi_1) , \quad (108)$$

$$D_{13}^{0k} = -\chi_{13}^k F_V^{(1)} + \mathbf{q} \times \Sigma_{13}^k F_V^{(2)} , \quad (109)$$

$$D_{13}^{mk} = \epsilon^{mrs} [(\Delta_{13}^r F_V^{(1)} + q^0 \Sigma_{13}^r + \phi_{13}^+ q^r F_V^{(2)}) \delta^{sk} - q^r (\Pi_3^s \Pi_1^k + \Pi_1^s \Pi_3^k) F_V^{(2)}] , \quad (110)$$

$$X_{24}^0 = \mathbf{k} \cdot \chi_{24} a_{46}^0 , \quad (111)$$

$$X_{24}^m = \mathbf{k} \cdot \chi_{24} a_{46}^m - \epsilon^{mrs} \Pi_2^r \Pi_4^s A_1 - \epsilon^{mrs} k^r \Delta_{24}^s A_2 , \quad (112)$$

$$\begin{aligned} Y_{24}^{0,l} &= (a_{35}^0 + k^0 A_2) \Delta_{24}^l - a_{46}^0 [k^0 \Sigma_{24}^l - \phi_{24}^- k^l + \Pi_2^l \Pi_4 \cdot \mathbf{k} - \Pi_4^l \Pi_2 \cdot \mathbf{k}] \\ &\quad - A_1 \Sigma_{24}^l + A_2 [k^l \phi_{24}^- + \Pi_2^l \Pi_4 \cdot \mathbf{k} + \Pi_4^l \Pi_2 \cdot \mathbf{k}] , \\ Y_{24}^{m,l} &= (a_{35}^m + k^m A_2) \Delta_{24}^l - a_{46}^m (k^0 \Sigma_{24}^l - \phi_{24}^- k^l - \Pi_2^l \Pi_4 \cdot \mathbf{k} - \Pi_4^l \Pi_2 \cdot \mathbf{k}) \\ &\quad - A_1 (\phi_{24}^- \delta^{ml} + \Pi_4^m \Pi_2^l + \Pi_2^m \Pi_4^l) - A_2 [\mathbf{k} \cdot \Delta_{24} \delta^{ml} - \Delta_{24}^m k^l \\ &\quad - k^0 (\phi_{24}^- \delta^{ml} + \Pi_4^m \Pi_2^l + \Pi_2^m \Pi_4^l)] . \end{aligned} \quad (113)$$

References

- [1] F. Plouin et al., Phys. Lett. **B276**, (1990) 526; and references therein.
- [2] A. M. Bergdolt et al., Phys. Rev. **D48**, (1993) R2969.
- [3] E. Chiavassa et al., Phys. Lett. **B322**, (1994) 270; Phys. Lett. **B337**, (1994) 192.
- [4] H. Calén et al., Phys. Lett. **B366**, (1996) 39.
- [5] U. Schubert, "The Reaction $pp \rightarrow pp\eta$ Close to Threshold", Ph.D thesis, Uppsala University, 1995.
- [6] S. Haggström, " Production of η -mesons in Proton-Neutron Collisions", Ph.D thesis, Uppsala University, 1997.
- [7] H. Calén et al., Phys. Rev. Lett. **79**, (1997) 2642.
- [8] B. Krushe et al., Phys. Lett. **B358**, (1995) 40.
- [9] B. Krushe et al., Phys. Rev. Lett. **74**, (1995) 3736.
- [10] P. Hofmann-Rothe et al., Phys. Rev. Lett. **78**, (1997) 4697.
- [11] L. C. Liu, J. T. Londergan and G. Walker, Phys. Rev. **C40**, (1989) 832.

- [12] J. F. Germond and C. Wilkin, Nucl. Phys. **A518**, (1990) 308.
- [13] J. M. Laget, F. Wellers and J. F. Lecomte, Phys. Lett. **B257**, (1991) 254.
- [14] T. Vetter, A. Engel, T. Biro and U. Mosel, Phys. Lett. **B263**, (1991) 153.
- [15] A. Moalem, E. Gedalin, L. Razdolskaja and Z. Shorer, Nucl. Phys. **A589**, (1995) 649.
- [16] A. Moalem, E. Gedalin, L. Razdolskaja and Z. Shorer, Nucl. Phys. **A600**, (1996) 445.
- [17] C. Wilkin, Phys. Rev. **C47**, (1993) R938.
- [18] M. Batinič, Ivo Šlaus, A. Švartc, and B. Neefkens, Phys. Rev. **C51**, (1995) 2310.
- [19] M. Batinič, Ivo Šlaus, and A. Švartc, Phys. Rev. **C52**, (1995) 2188.
- [20] J.-F. Germond and C. Wilkin, **G15**, (1989) 437.
- [21] S. A. Rakitiansky, S. A. Sofianos, M. Braun, V.B. Belyaev and W. Sandhas, Phys. Rev. **C47**, (1997).
- [22] M. Benmerrouche and N. C. Mukhopadhyay, Phys. Rev. Lett. **67**, (1991) 1070.
- [23] G. Fäldt and C. Wilkin, Nucl. Phys. **A587**, (1995) 769.
- [24] G. Fäldt and C. Wilkin, Nucl. Phys. **A604**, (1996) 441.
- [25] J. Piekarewicz et al., Phys. Rev. **C55**, (1997) 2571.
- [26] M. P. Rekalo, J. Arvieux, and E. Tomasi-Gustafson, Phys. Rev. **C55**, (1997) 2630.
- [27] R. M. Brown et al. , Nucl. Phys. **B153**, (1979) 89.
- [28] Particle Data Group, J. J. Hernandez et al. , Phys. Rev. **D50** (1994) 1173.
- [29] R. Machleidt. Adv. in Nucl. Phys. **19**, (1989) 189.

- [30] S. Gaziorovitch, "Elementary Particle Physics", J. Willey, N.Y.,1969, p. 364.
- [31] C. Itzykson, J. B. Zuber, "Quantum Field Theory", McGraw-Hill, N.Y. 1980, Vol. 1 p. 360., Vol. 2 p. 384.
- [32] T. Ericson and W. Weise, "Pions and Nuclei", Clarendon Press, Oxford, 1988, p. 480.
- [33] E. Byckling and K. Kajantie, Particle Kinematic (Wiley, London, 1973).
- [34] A. Moalem, L. Razdolskaja, E. Gedalin, hep-ph/9505264 and to be published; see also A. Moalem, E. Gedalin, L. Razdolskaja and Z. Shorer, π N Newsletter Proceeding of the 6th International Symposium on Meson-Nucleon Physics and the Structure of the Nucleon, **10**, (1995) 172.
- [35] H.P.Noyes, Ann. Rev. Nucl. Sci., **22** (1972) 465.
- [36] A. Moalem, E. Gedalin and L. Razdolskaja, to be published.
- [37] L. Tiator, C. Bennhold, and S. S. Kamalov, Nucl. Phys. **A580**, (1994) 455.

Table 1: The model parameters. The constants g_{BNN} , cut off parameters (Λ_B) and meson masses (m_B) are taken from Machleidt et al.[29]; their relativistic OBEP solution with pseudoscalar coupling for π and η and with $f_{\rho NN}/g_{\rho NN} = 6.1$, $f_{\omega NN}/g_{\omega NN} = 0$.

	$m_B(MeV)$	$g_{BNN}^2/4\pi$	$\Lambda_B(MeV)$	g_{BNN^*}
π	138	14.6	1300	0.8
σ	550	8.03	1800	0.5 ^{b)}
η	547.3 ^{a)}	3.0	1500	2.2
ρ	769	0.95	1300	1.66
ω	783	20.0	1500	0.94 ^{b)}
δ	983	5.07	1500	1.48 ^{c)}

^{a)} From Ref.[1].

^{b)} From $g_{\sigma NN^*}/g_{\sigma NN} = g_{\pi NN^*}/g_{\pi NN}$

^{c)} From $g_{\delta NN^*}/g_{\delta NN} = \frac{1}{2} [g_{\pi NN^*}/g_{\pi NN} + g_{\eta NN^*}/g_{\eta NN}]$

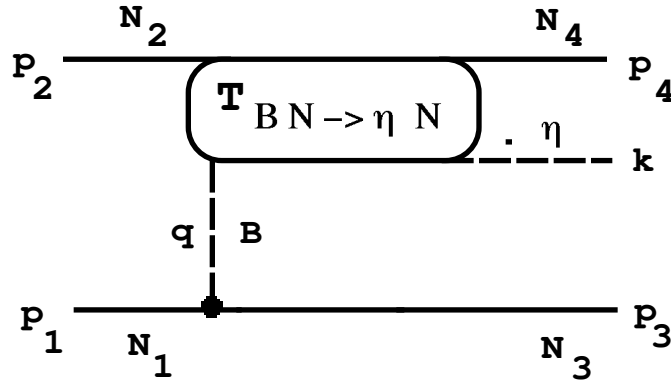


Figure 1: The primary production mechanism for the $NN \rightarrow NN\eta$ reaction. A boson B created on nucleon 1 (momentum p_1), is converted into an η meson (momentum k) on nucleon 2 (momentum p_2).

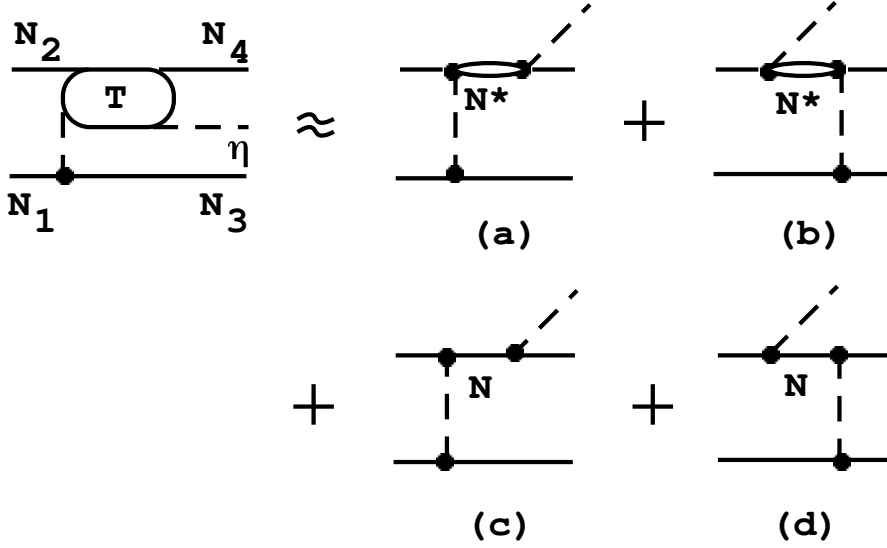


Figure 2: Feynman diagrams for η meson production in NN collisions. (a) s-channel N^* pole contribution; a boson B (dashed line) formed on nucleon 1 (momentum p_1) is absorbed on nucleon 2 (momentum p_2) which is excited to an isobar state with momentum $p = k + p_4$ which then decays into a nucleon 4 (momentum p_4) and an η meson (momentum k). (b) u-channel N^* pole; pre-emission counter part of diagram (a) where an η meson is emitted before collision. (c) s-channel N pole; as in (a) with a nucleon in the intermediate state. (d) u-channel N pole contribution; pre-emission counter part of (c). There are four more graphs in which the exchanged boson is formed on nucleon 2. These are not displayed here but their contributions are included in the calculations.

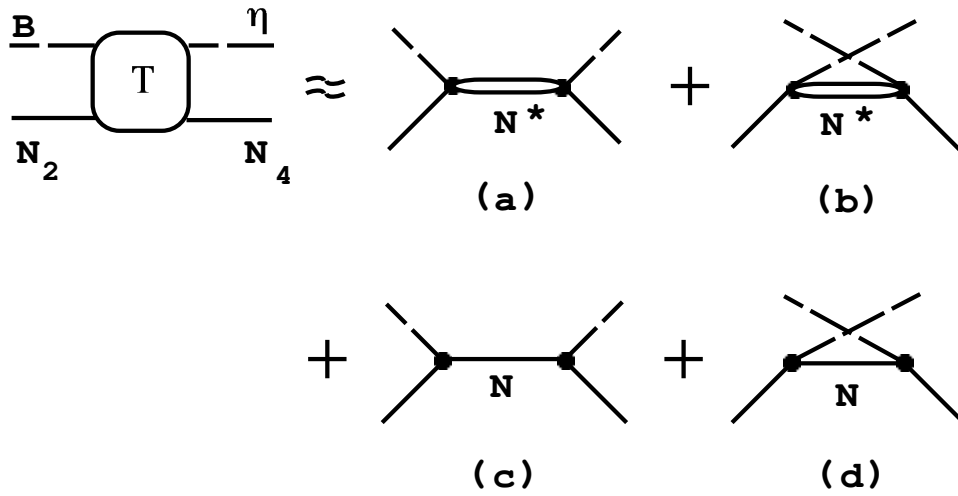


Figure 3: Feynman diagrams for the conversion process $BN \rightarrow \eta N$ (a) s-channel N^* pole contribution, (b) u-channel N^* pole; pre-emission counter part of diagram (a), (c) s-channel N pole; as in (a) with a nucleon in the intermediate state. (d) u-channel N pole contribution; pre-emission counter part of (c).

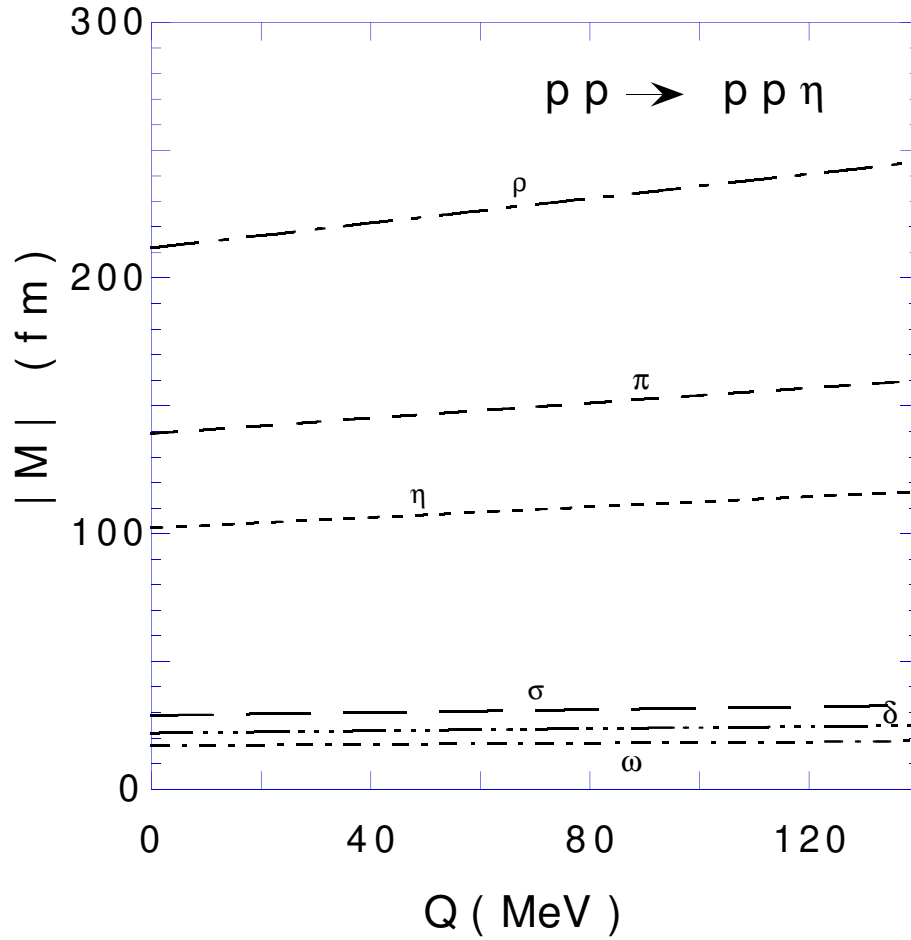


Figure 4: Partial exchange amplitude for the $pp \rightarrow pp\eta$ reaction. The ω contributions from s and u-channels with N^* poles cancel out and M_ω is very weak (see text).

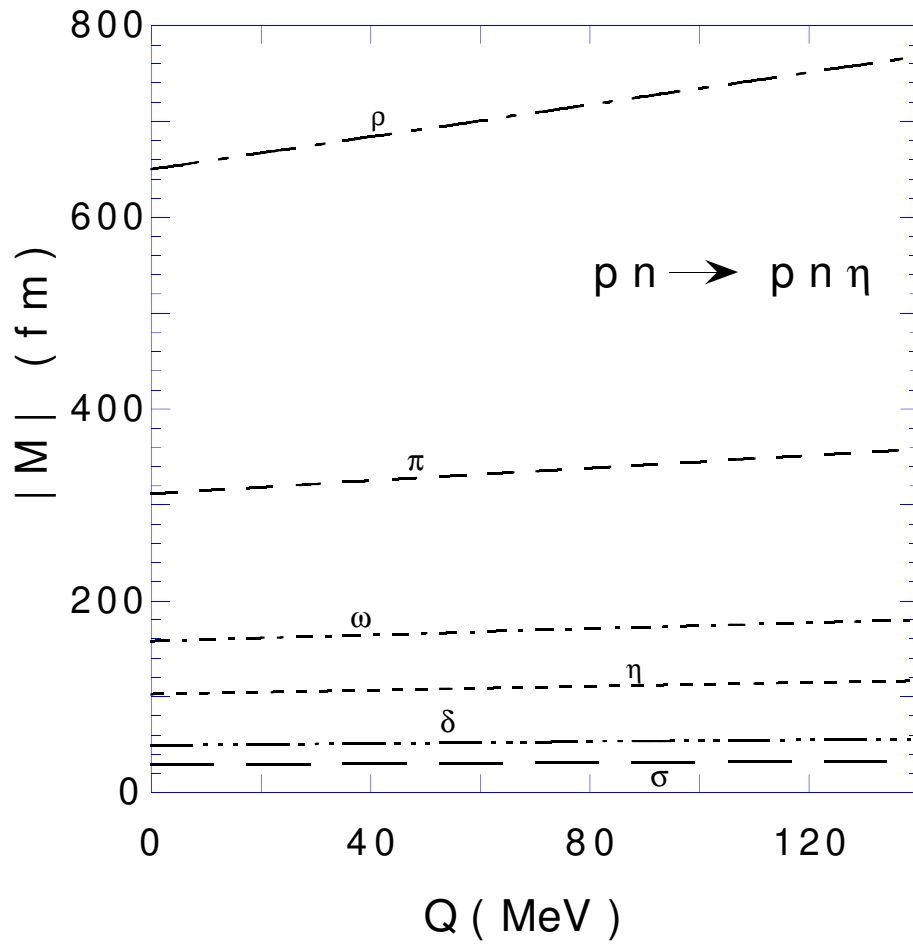


Figure 5: Partial exchange amplitude for the $pn \rightarrow pn\eta$ reaction.

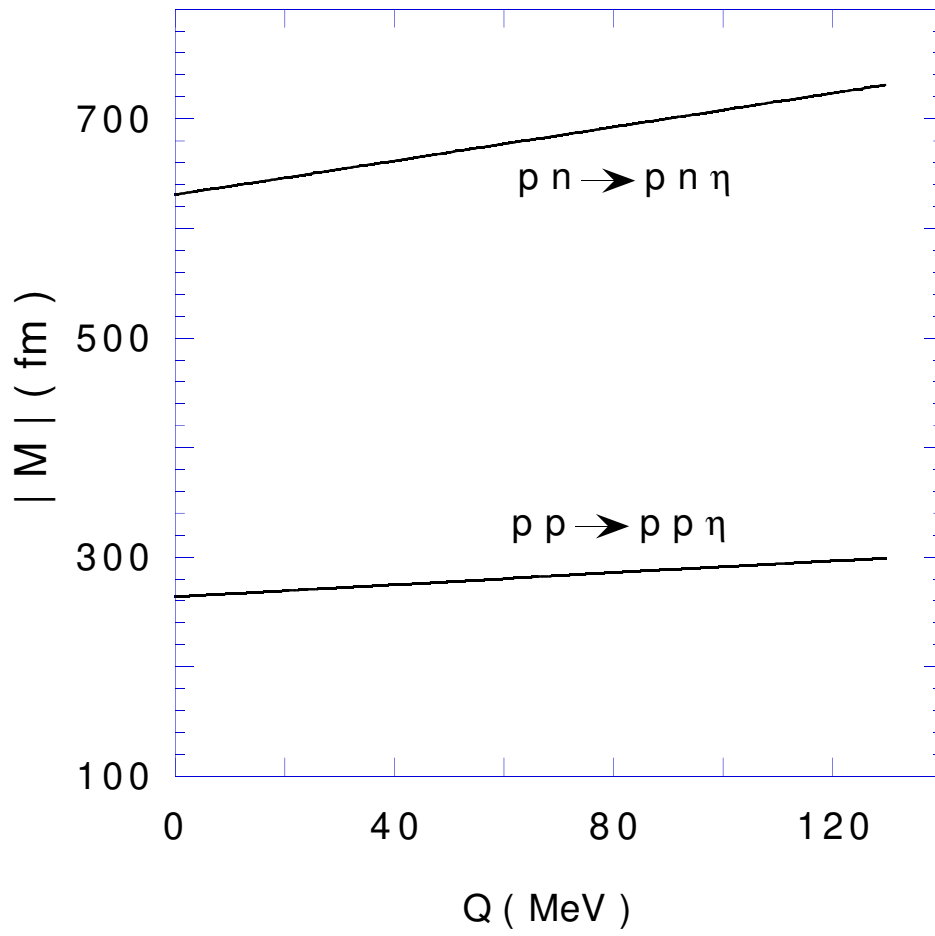


Figure 6: Primary production amplitude for the $pp \rightarrow pp\eta$ and $pn \rightarrow pn\eta$ reactions with all of the relative phases taken to be +1 (our standard solution).

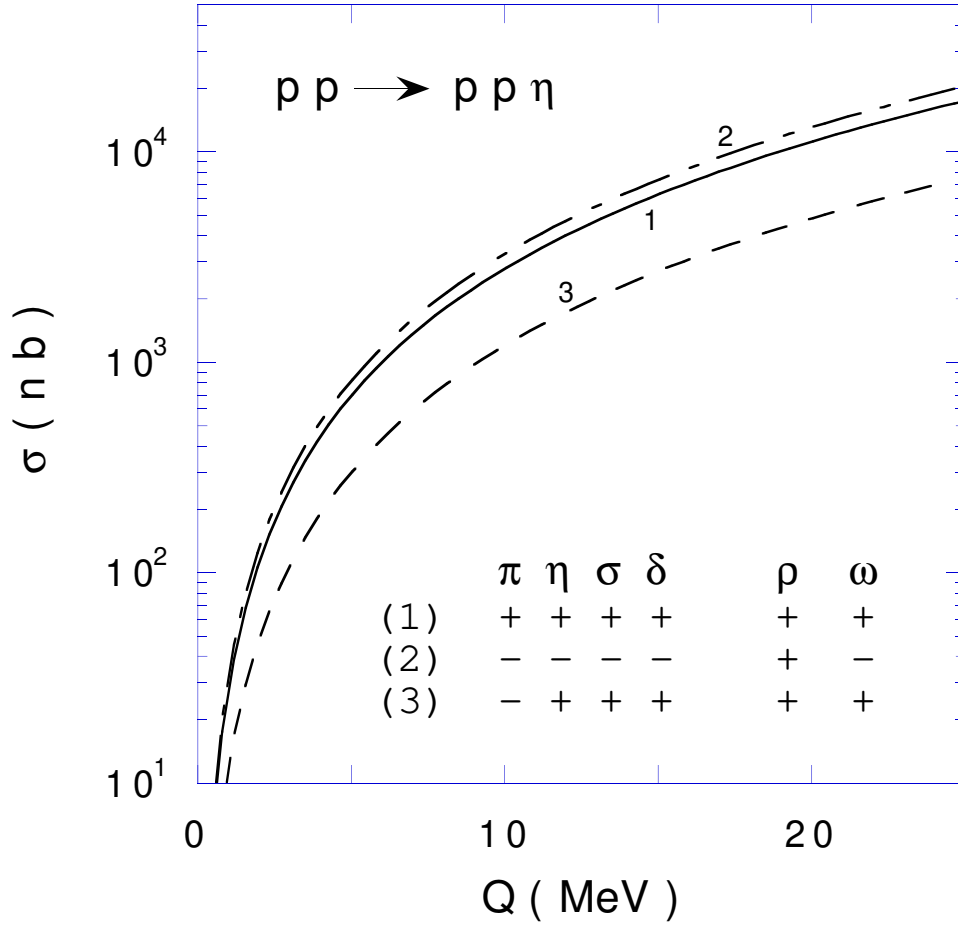


Figure 7: Predictions for the $pp \rightarrow pp\eta$ cross sections near threshold with different phase combinations. The solid line displays the standard solution. The lowest (dashed curve) and the highest (dash-dotted curve) cross sections are obtained with the $\pi, \eta, \sigma, \delta, \rho$ and ω relative phases being $-++++$ and $-----+-$, respectively.

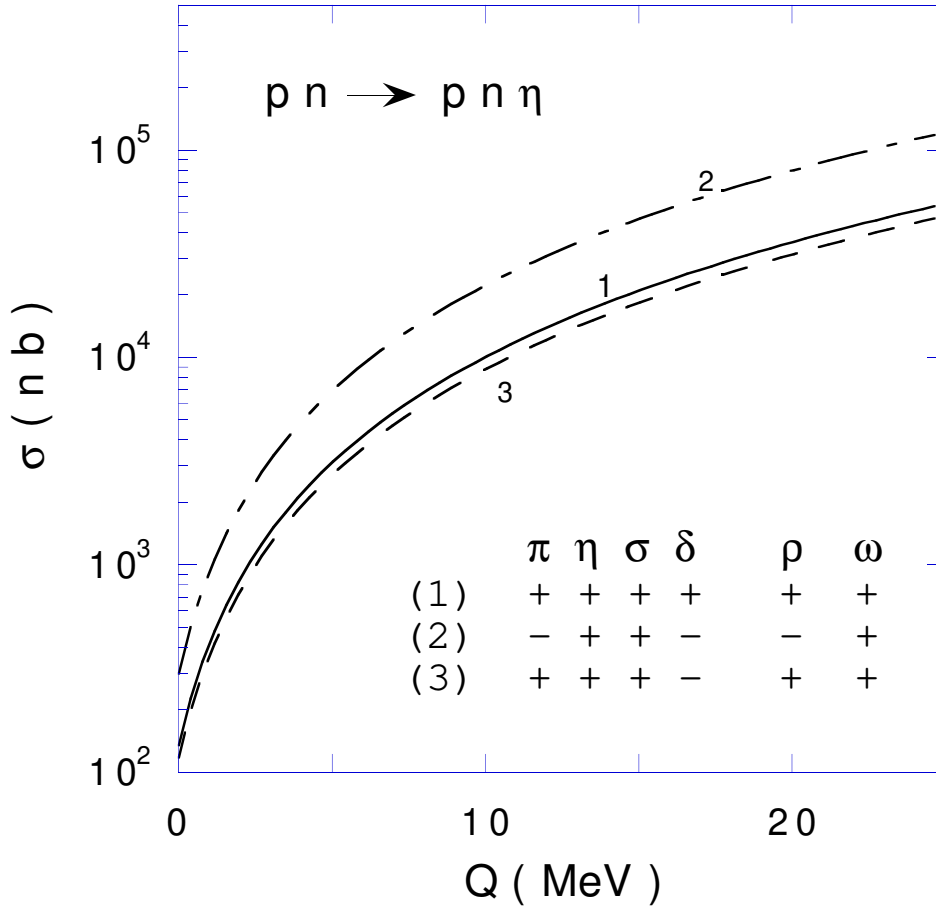


Figure 8: Predictions for the $pn \rightarrow pn\eta$ cross sections near threshold with different phase combinations. The solid line displays the standard solution. The lowest (dashed curve) and the highest (dash-dotted curve) cross sections are obtained with the $\pi, \eta, \sigma, \delta, \rho$ and ω relative phases being $+++--+$ and $-++--+$, respectively.

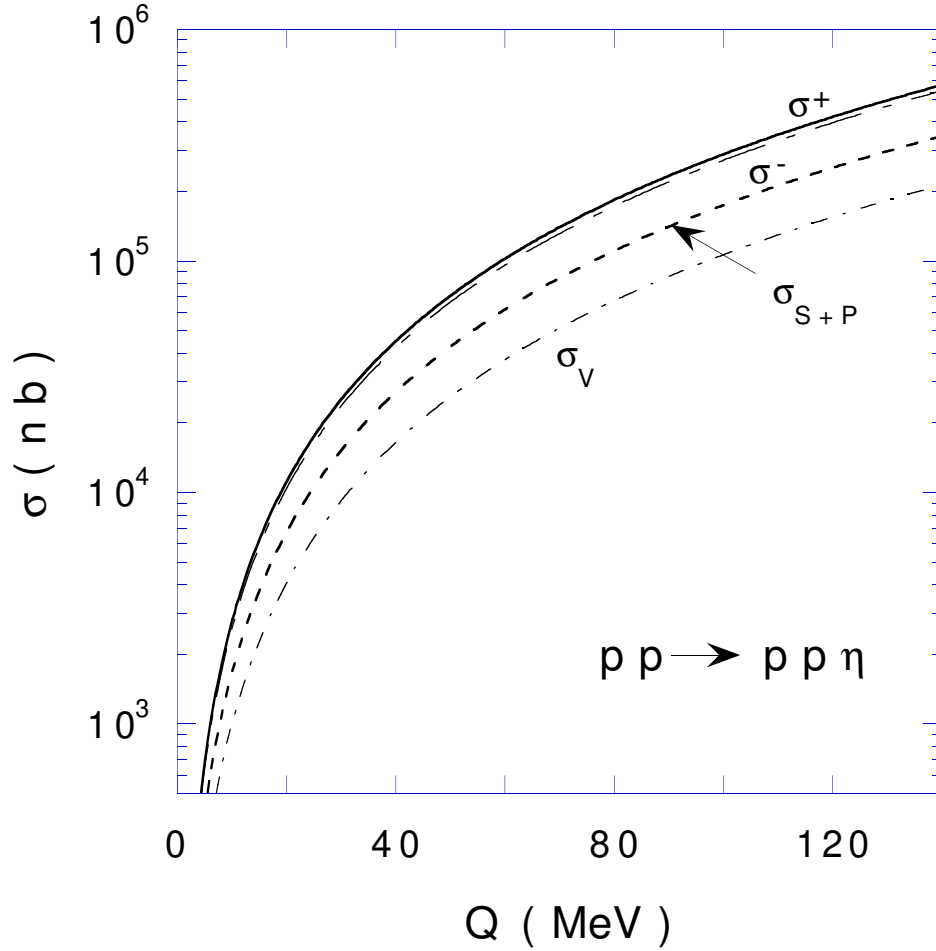


Figure 9: Interference between vector and scalar-pseudoscalar meson contributions. The curves labeled by σ_V, σ_{P+S} , represent partial cross sections with vector meson exchanges and with scalar plus pseudoscalar exchanges only. The other lines are total cross sections with all the relative phases taken as +1 (σ^+) and with the same relative phases for the scalars and pseudoscalars except for M_ρ and M_ω having the opposite sign (σ^-).

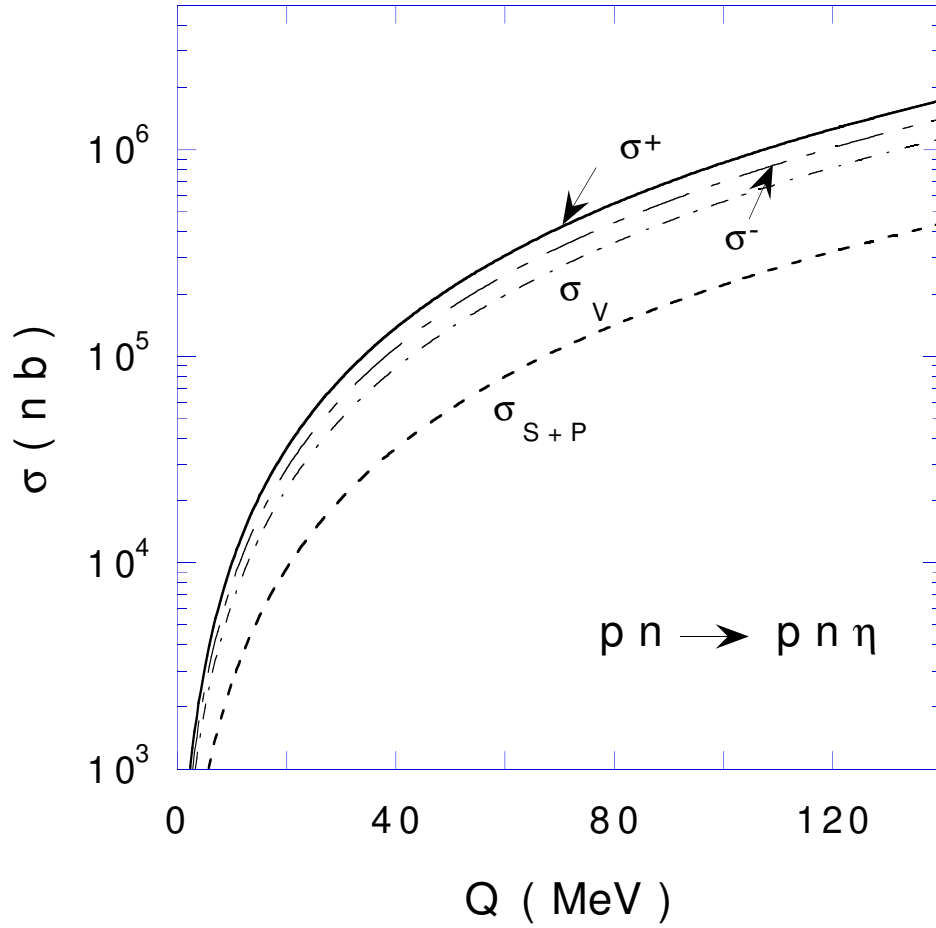


Figure 10: Interference between vector and scalar-pseudoscalar meson contributions for the $pn \rightarrow pn\eta$ reaction. See captions of Fig. 9.

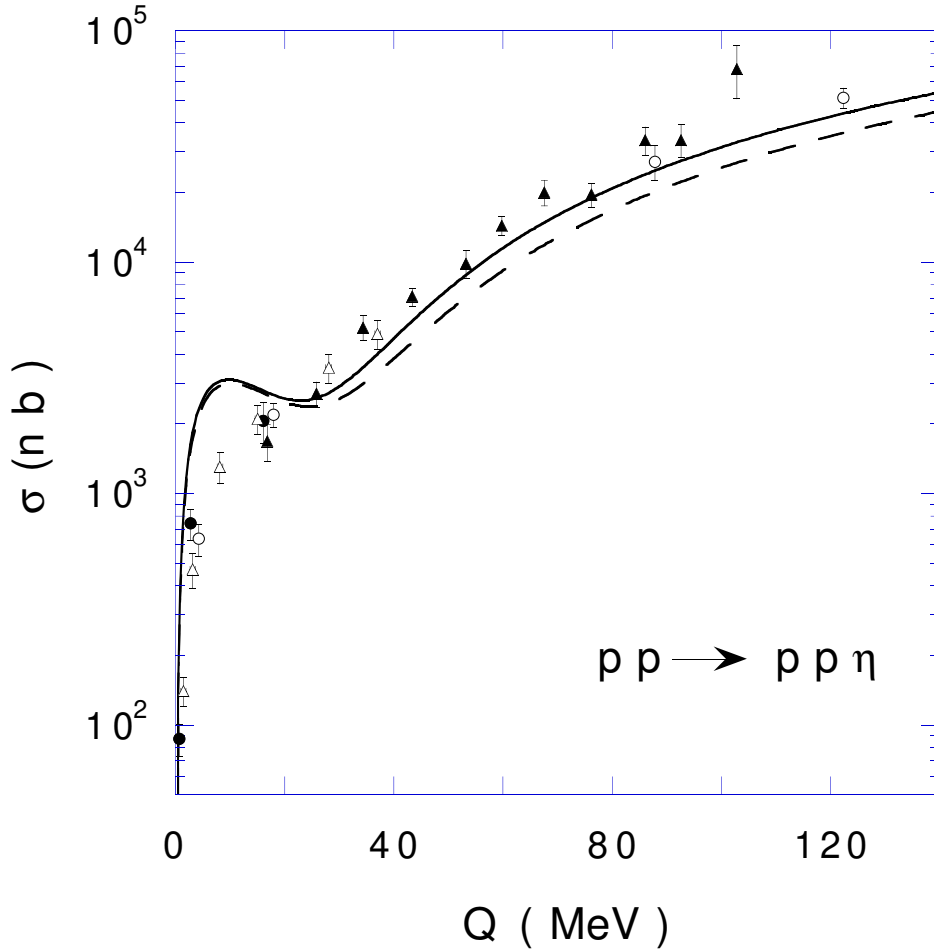


Figure 11: Energy integrated cross sections for the $pp \rightarrow pp\eta$ reaction *versus* the energy available in the CM system. All curves include FSI corrections via the approximation Eqn. 77. Predictions are given for the standard solution with both resonance and background terms included (solid line) and with the resonance term only (dashed curve). The dot-dashed curve (which in this case override the solid line) gives the standard solutions as obtained with $g_\omega = 0$. The data shown are taken from Refs. 2-4,7.

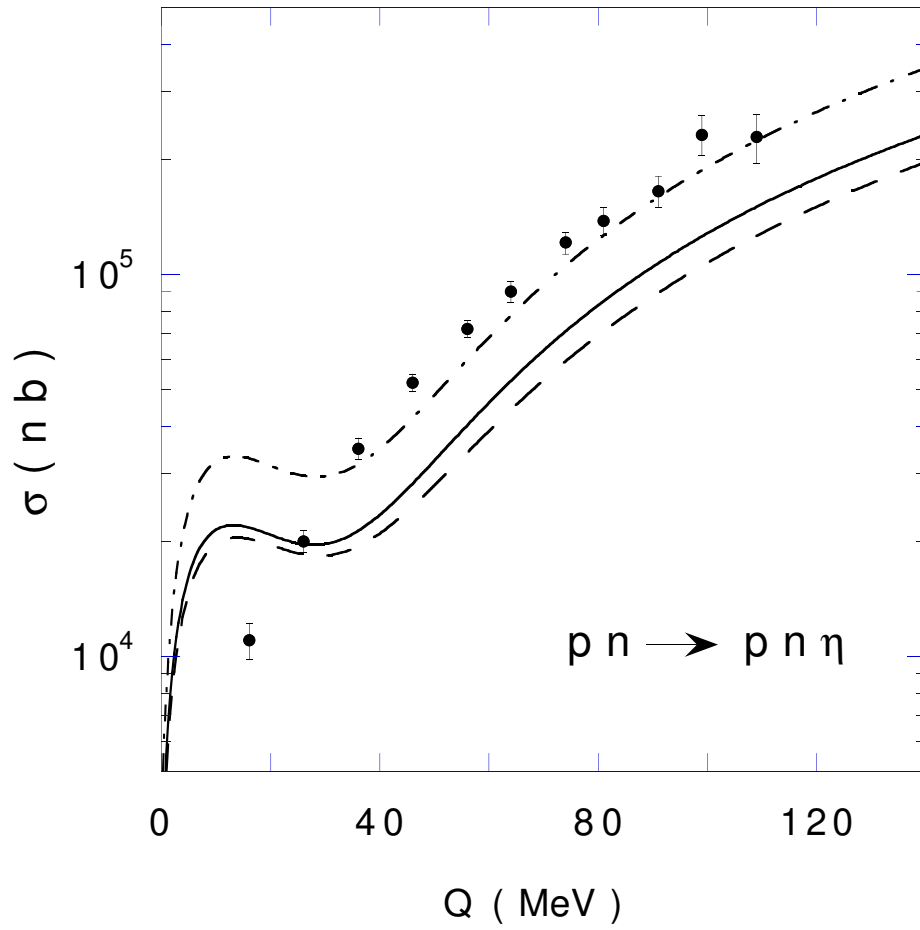


Figure 12: Energy integrated cross section for the $pn \rightarrow pn\eta$ reaction. Data point are taken from Ref. 7. See caption of Fig. 11.

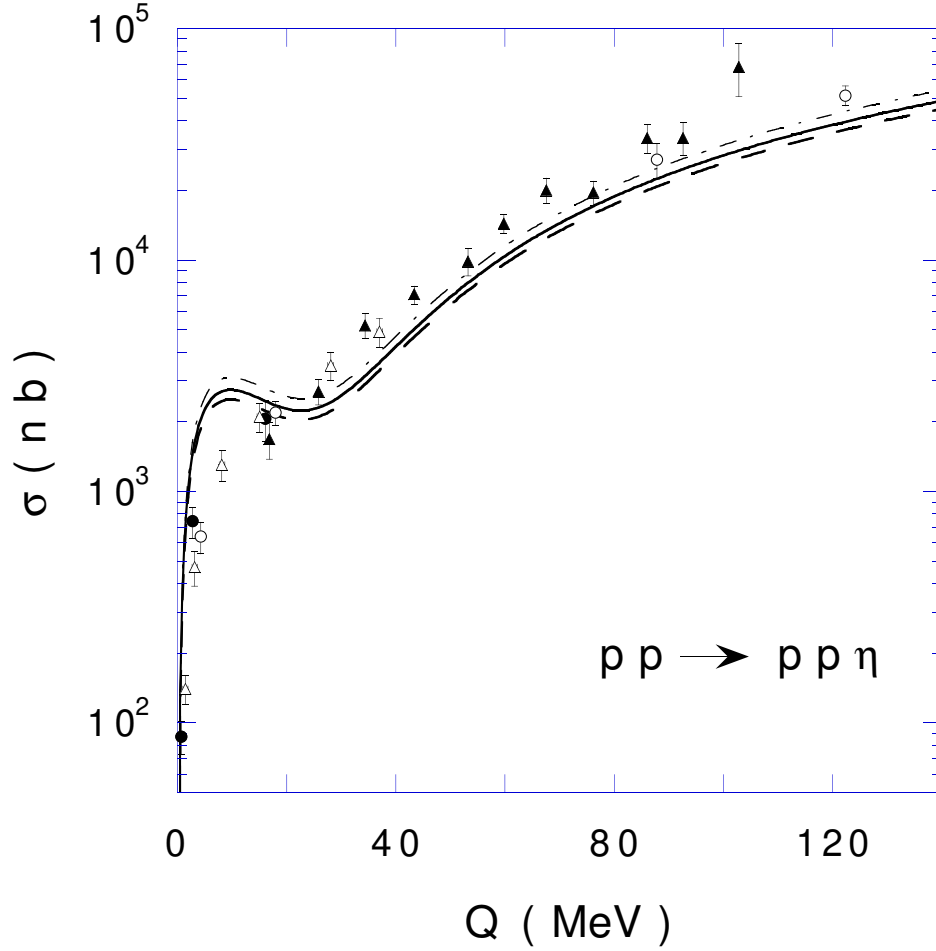


Figure 13: Effects of ω , σ , δ exchanges. Predictions for the $pp \rightarrow pp\eta$ cross section are given for the standard solution with (i) $g_{\omega NN^*} = 0$ (solid line), (ii) $g_{\omega NN^*} = g_{\sigma NN^*} = 0$ (dashed curve) and (iii) $g_{\omega NN^*} = g_{\sigma NN^*} = g_{\delta NN^*} = 0$ (dash-dotted curve).

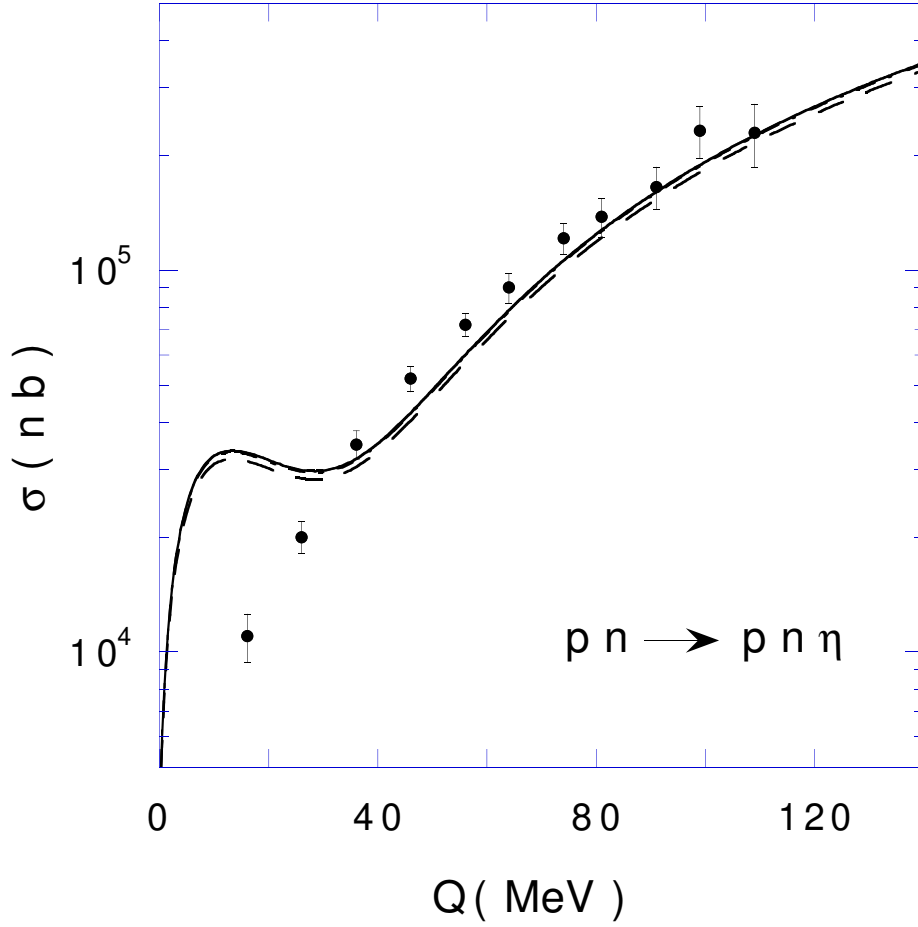


Figure 14: Effects of ω, σ, δ exchanges. Predictions for the $pn \rightarrow pn\eta$ cross section are given for the standard solution with (i) $g_{\omega NN^*} = 0$ (solid line), (ii) $g_{\omega NN^*} = g_{\sigma NN^*} = 0$ (dashed curve) and (iii) $g_{\omega NN^*} = g_{\sigma NN^*} = g_{\delta NN^*} = 0$ (dash-dotted curve).

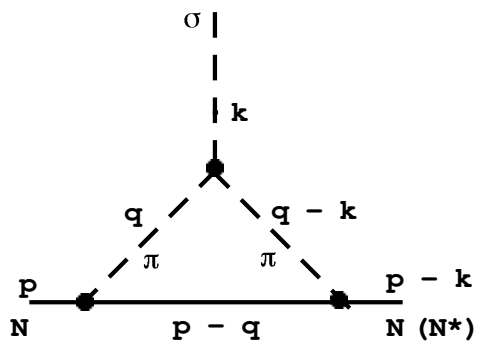
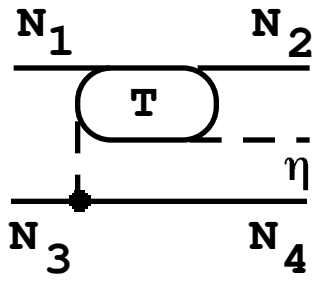
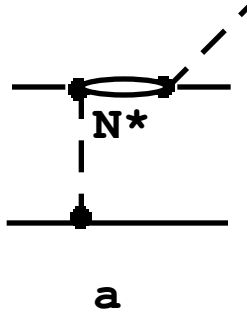


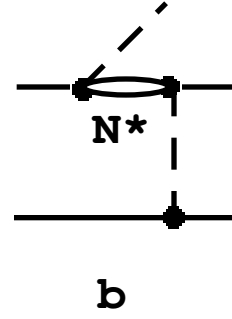
Figure 15: An effective triangle diagram used to derive an expression for $g_{\sigma NN^*}$



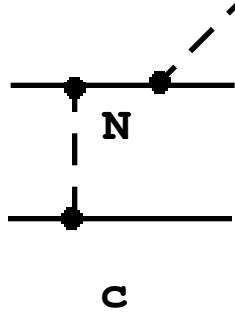
\approx



+



+



+

